Solar PV and EV Controls for Reactive Power Support on Large Distribution Systems Modeled with Experimental and Synthetic Loads

Rosemary E. Alden[1], *Student Member, IEEE*, Malcolm McCulloch[2], *Senior Member, IEEE*, and Dan M. Ionel[1], *Fellow, IEEE*

[1]SPARK Laboratory, Stanley and Karen Pigman College of Engineering, University of Kentucky, Lexington, KY, USA
[2]EPG, Department of Engineering Science, University of Oxford, Parks Road, Oxford, OX1 3PJ, UK
rosemary.alden@uky.edu, malcolm.mcculloch@eng.ox.ac.uk, dan.ionel@ieee.org

***Abstract*—Changes to electric power distribution equipment may be needed to adapt to distributed energy resources (DERs) such as solar photovoltaic (PV) generation and electric vehicle (EV) batteries. Within this paper, an optimization methodology for reactive power support (RPS) controls managed by utilities for EV bi-directional charger power factor and improve substation power quality and voltage across the system is proposed. An IEEE benchmark distribution system, the 123 node test feeder, is modified to include 1,765 experimental residential profiles at typical, high resolution of 15min from smart meters, solar PV generation calculated from weather data, and EV modules based on driver behavior surveying. Two cases for RPS controls for EVs are investigated: 1) vehicle-to-grid (V2G) injection to counteract leading power factor (pf) at the main substation and 2) EV charging to improve substation pf and to avoid unacceptable system bus voltage rise. The results illustrate the benefits of RPS, which address major challenges of EV adoption.**

***Index Terms*—Reactive power compensation, Virtual Power Plant (VPP), Smart Meter, Smart Grid, Distributed Energy Resources (DERs)**

I. Introduction

This paper aims to answer the question if reactive power support (RPS) from electric vehicle (EV) bi-directional chargers may improve distribution system operation including bus voltages and losses through substation power factor. This contribution is important for utilities as they make decisions involving EV adoption and infrastructure upgrades to system equipment such as smart capacitors. With the implementation of RPS from EV bi-directional EV chargers in vehicle-to-grid (V2G) and grid-to-vehicle (G2V), updates to industry practices for power factor (pf) control with capacitors and load tap changing devices may be reduced.

The concept of RPS has been applied to distributed energy resources (DERs) such as for solar photovoltaic (PV) reactive power sharing with smart inverters and distributed control strategies in microgrid applications to improve voltage [1]. National laboratories have emulated virtual power plant (VPP) operation of solar PV for RPS as power hardware-in-the-loop (PHIL) with load tap changing devices and bus voltages [2]. Early studies into RPS from EVs focused on the effectiveness of the phase angle adjustment during solar PV transients on a small power system model [3].

Another notable study into RPS from EVs focused responding to sudden increases in load with V2G discharging in real time [4]. Further use cases for RPS from decentralized EVs were described and simulated on an IEEE 33 node test feeder by U.S. national laboratories and universities to improve costs as well as increase the number of EV chargers [5]. During EV charging operation, RPS was considered more frequently, such as with model predictive controls across the IEEE 123 node test feeder to avoid solar PV curtailment at the hourly resolution [6].

Very recent papers account for EV charging scheduling within the four quadrants to provide voltage regulation, saving energy through CVR [7], [8]. The first of these studies employs RPS to better utilize renewable energy resources and machine learning to control the active and reactive power. The latter demonstrates that RPS improves voltages further than tap change settings alone and reduces system losses. Coinciding with the research into the grid impacts of EV RPS, development of EV bi-directional chargers capable of phase angle control into all four quadrants has been experimentally demonstrated [9].

The main contributions of this work include proposal of an optimization methodology for minute-to-minute (M2M) controls of EV power factor for RPS and modeling of a large-scale distribution system (DS) with over 1700 experimental smart meter profiles from one of the largest rural field demonstrators in the USA. The developed co-simulation framework for VPP case studies with solar PV and EVs employs representative combined experimental and synthetic smart meter profiles, reported EV driving behavior, and weather data. Minutely simulation of V2G and G2V with RPS controls for optimized substation pf result in improved losses and system voltages. They address a gap in the literature to quantify the benefits of EV based RPS in a scalable manner at high resolution across a multi-hour control period such as could be enacted as a program by a utility.

II. Distribution System with Residential Loads, EV, and PV

Open-source large distribution system power flow models at low voltage with experimental residential profiles are not commonly publicly available due to security regulations and practices with private data of consumers. To provide a realistic residential neighborhood for RPS studies, the IEEE 123 node test feeder was modified (Fig. 1) to include experimental smart meter profiles from the SET project, one of the largest rural data sets with 5,000+ home at 15min resolution from Glasgow, KY, USA [10]. The IEEE 123 node test feeder is a 4.16kV

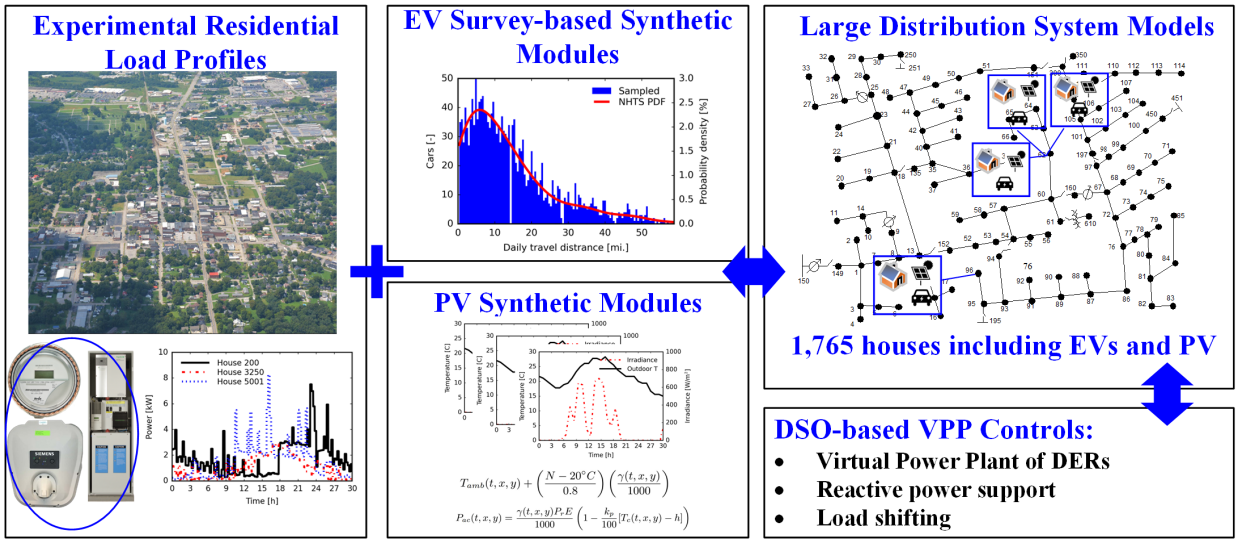

Fig. 1. For use in VPP studies, the IEEE 123 node test feeder has been modified to include experimental residential load profiles at 15min resolution from Glasgow, KY and the SET field project. Synthetic modules for EVs and solar PV based on a national survey of human driving patterns and weather data from the same region.

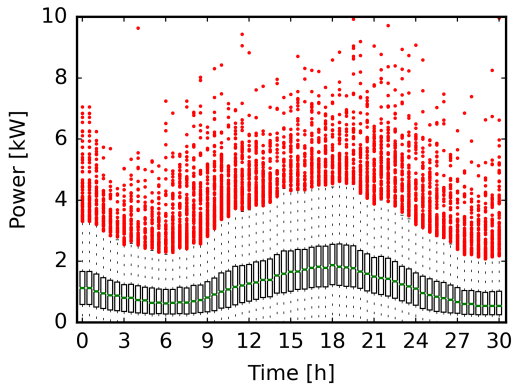

Fig. 2. The box and whisker plot for the 1,765 daily load profiles from the SET field project shows expected high variation, with outlier points from high powered appliances, such as electric water heaters throughout the day.

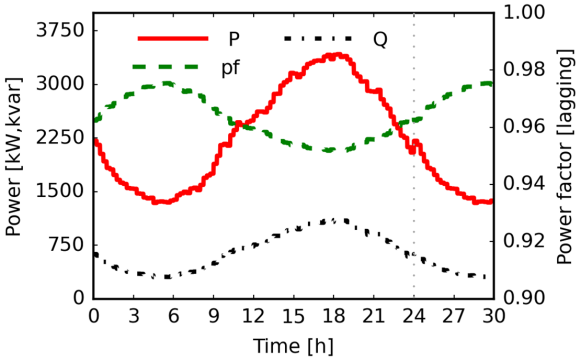

Fig. 3. The aggregate load of the modified IEEE 123 test feeder, which includes thousands of experimental profiles from the SET field project, is within expected ranges for peak load and power factor at the main substation.

system with three phase and two phase loads fed from a 5MVA wye to wye transformer, which represents the main feeder.

One house profile was added in place of 2.5kW of the original load at each node, i.e. 1,765 house profiles. A summer day was selected for the house profiles, and the high variability of residential total load has been visualized in Fig. 2. Within each time increment the distribution of the load of the 1,765 houses has been separated into quadrants with the mean marked by the center green line. The outliers shown as red dots may be partially explained by short-duration high power appliances such as electric water heaters (EWHs).

Synthetic modules for solar PV generation from weather input data and EV battery state of charge (SOC) based on the 2017 National Household Travel Survey (NHTS) were added across the DS [11]. The synthetic EV modules contain a daily driving distance, home arrival time, and calculated SOC upon arrival from experimental survey responses in the US states of KY and TN and the Gaussian Kernel Density Estimator methods described in [12]. Each synthetic battery is assumed to have a 100kWh capacity, 10kW bi-directional charger, and round trip efficiency of 85%. The solar PV residential modules were randomly selected between 3-7.5kW. The DS was simulated by OpenDSS power flow software through the python API with synthetic EV and PV modules. The dss-python library served as the API connection to OpenDSS within the optimization cost function [13], as described further in Section IV.

The residential load profiles and synthetic EV and PV modules were added to the system by editing the power in kW and pf of each node iteratively every minute. Tap control settings were evaluated every iteration in voltage regulators and transformers across the DS. A 600kvar capacitor was removed to prevent a substation leading pf during the new low load at night. Following the modifications, the main substation aggregate power matches the original load of 3.6MW at peak time, and the 0.93-0.98 lagging pf was considered within acceptable range for a substation transformer (Fig. 3).

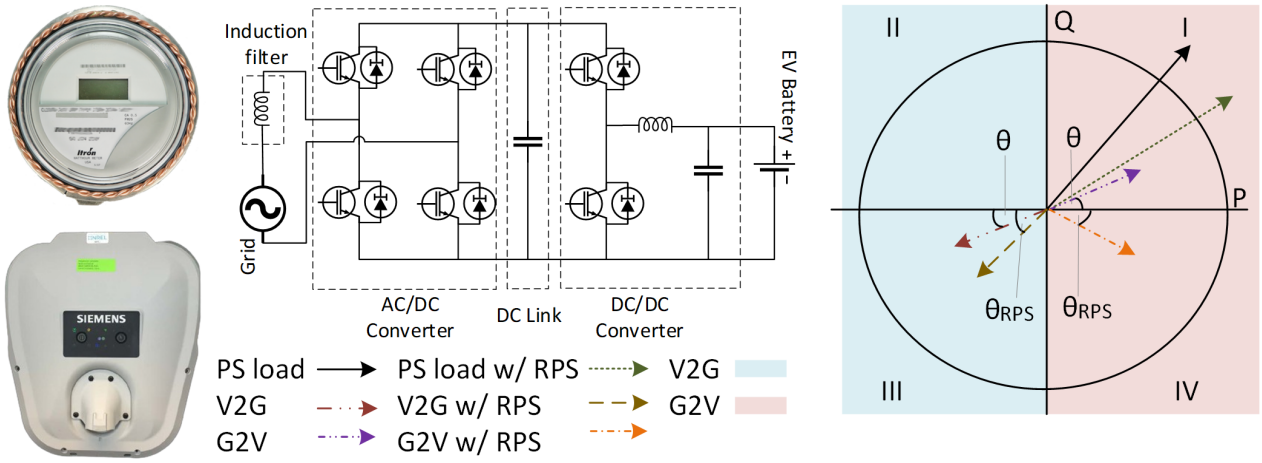

Fig. 4. Commercially available bi-directional EV chargers and smart meters may enable coordinated G2V and V2G operation across distribution systems. Example reactive power support (RPS) for both G2V and V2G cases shown with AC/DC converter phase angle shifts. Controls from the utility perspective for RPS to improve the substation pf and bus voltages may mitigate system strain from additional charging load or DER generation.

III. Power Factor Correction with Smart Capacitors and EVs

Across multiple EV charger typologies and companies, bi-directional EV chargers offer the capability to operate the battery in vehicle-to-grid (V2G) as well as charging mode, grid-to-vehicle (G2V) [14]. In Fig. 4, an example power electronic converter for a bi-directional EV charger and the phasor diagram for RPS from the perspective of the main feeder transformer were visualized. The AC/DC converter may be controlled to change the phase angle and subsequent reactive power.

The historical and industry convention is to size fixed distribution system capacitors was based on light load magnitude at night [15]. This practice does not account for very low load or reverse radial power flow from highly variable solar PV generation that suddenly may drop or increased EV charging load at night. Due to higher load variability from solar PV and EV charging at night, including reactive power spikes, the operation of more switch capacitors that turn on or off may be required. The replacement of fixed capacitors with smart capacitors is actively being considered across utilities in the US. For example, a public document from Central Hudson Gas & Electric in New York describes the upgrade of 360 distribution system fixed capacitors to smart capacitors to avoid overcompensation during off-peak times [16].

The initiative was scheduled for 2010 and cost $7.2 million USD. Since this time, more distribution systems may benefit from or require such upgrades as the adoption rate of new technologies increases and efforts to reduce cost should be considered. Even once smart capacitors are installed, the maximum times they may change state, whether this is sufficient to mitigate voltage violations from EV charging load or solar, and RPS controls to further improve the DS performance should be explored. Because solar PV generation technology has been deployed in greater numbers without automated RPS controls, EV-based RPS was selected for case studies.

The IEEE 123 node test feeder was simulated over a sunny summer day with varied penetrations of solar PV generation (Fig. 5). The addition of solar PV improves the main feeder and transformer pf at low penetration rates, and it causes a leading pf at high penetration, e.g. 50%. This occurs because the low off-peak reactive power was reduced by solar PV generation to below the kvar injected by fixed capacitors, originally intended to improve voltage at night. This solar PV hosting study shows the need for RPS methods to accompany DERs as explored further in the case study.

IV. EV Reactive Power Support in Steady State Power Flow

Within the DS framework, the load active power, $P_i = S_i \angle \theta_i$ and pf, for each node, i, required by OpenDSS to solve the power flow was calculated employing the following system of equations:

$$\overbrace{S_i \cos\theta_i}^{P[kW]} = \sum_{j=0}^{k} S_j \cos\theta_j, \forall i \in \{1, 2, ..., N\}, \quad (1)$$

$$\overbrace{S_i \sin\theta_i}^{Q[kvar]} = \sum_{j=0}^{k} S_j \sin\theta_j, \forall i \in \{1, 2, ..., N\}, \quad (2)$$

where k is the max number of loads or generation sources including multiple houses at node i, and N the total number of nodes. Appliances and EV charging were considered the loads while PV and EV discharging as equivalent generators.

In this formulation, the residential house loads from the SET project and the solar PV generation were assumed to have a pf of 0.95 lagging. The EV bi-directional charger pf may be treated as a variable for phase angle controls and reactive power support. A M2M control scheme is proposed to optimize the DS pf at the main substation and minimize bus voltage violations outside 0.95-1.05p.u. by changing phase angle and subsequent pf for the EVs. For each node with multiple houses, the new phase angle and apparent power,

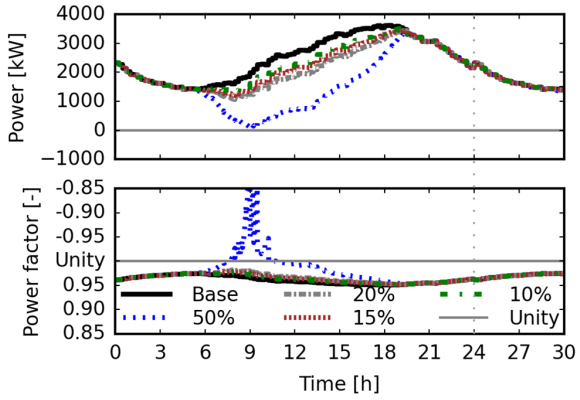

Fig. 5. Solar PV penetration varied from 10-50% on the IEEE 123 node test feeder illustrates a future smart grid scenario with reverse radial power flow where the substation power factor becomes leading.

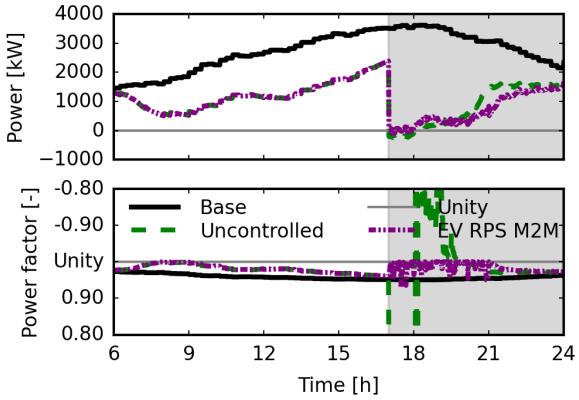

Fig. 6. Operation of bi-directional chargers in V2G for 670 EVs, approximately 40% of the houses, and 20% penetration of solar PV during the day. The uncontrolled case includes reverse radial power flow and leading power factor at the main substation, which the RPS corrects to near unity pf.

including variable EV power factor, for RPS was calculated as:

$$\theta_i = \arctan\left[\frac{S_{EV}\sin(\theta_{EV}) + S_{H,PV}\sin(\theta_{H,PV})}{S_{EV}\cos(\theta_{EV}) + S_{H,PV}\cos(\theta_{H,PV})}\right], \quad (3)$$

$$S_i = \frac{S_{EV}\cos(\theta_{EV}) + S_{H,PV}\cos(\theta_{H,PV})}{\cos(\theta_i)}, \quad (4)$$

where S_{EV}, θ_{EV} and $S_{H,PV}, \theta_{H,PV}$ are the apparent powers and phase angles of the EV and the house load with solar PV generation included.

The M2M controls for the phase angle of the bi-directional EV chargers may be determined through optimization following:

$$\min\Big[U - PF_M(t, C_{EV,\mathcal{Z}_i}) \times [-\eta_{pf}\eta_v]\Big], \quad (5)$$

where U represents unity power factor as 1.0, $PF_M(t, C_{EV,\mathcal{Z}_i})$ the substation power factor as a function time, t, and $C_{EV,\mathcal{Z}_i}$ which is the design selected for the set of EV bi-directional charger power factors across the distribution system, η_{pf} the penalty for a leading main substation power factor, and η_v the penalty for each voltage violation.

For the case studies contained in this paper, the differential evolution algorithm was applied. The co-simulation framework was developed in python, and the pymoo library was utilized for the optimization [17]. The distribution system power flow was considered directly in the solution of the cost function for over 1,000 design candidates of EV charger pfs across DS zones for each minute in the simulation.

To reduce solution time to approximately 1h and the number of independent variables from hundreds, i.e. one EV bi-directional charger per house, groups of houses connected across the distribution system are controlled in *zones*. For the example modified IEEE 123 node test feeder, the zones were selected to match the original 91 loads with a range of 10-150 houses per zone. Each house in the zone may or may not have an EV depending on the selected penetration level. Thus, the design solution set from the optimization is of the form:

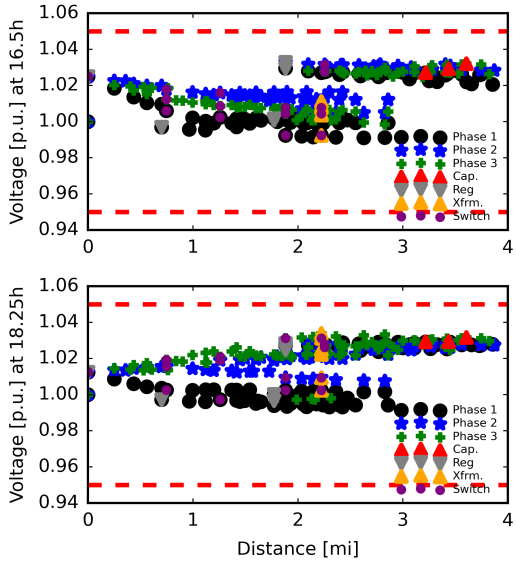

Fig. 7. The voltage across the system before V2G (top) and during V2G with RPS (bottom). System voltage rise may be partially explained from reduced loading on the system with the EV batteries acting as decentralized generation sources. Prevention of voltage violations were considered in the RPS controls.

$$C_{EV,\mathcal{Z}_i} \in \{PF_{lag}, -PF_{lead}\} \quad \text{of size } \mathcal{Z}, \quad (6)$$

where pf_{lag} and pf_{lead} are independent variable bounds per case study and $\mathcal{Z}$ is the number of zones selected across the distribution system, i.e. 91 in the example cases.

The bi-directional EV charger phase control to provide reactive power support into the second and fourth quadrant during charging and discharging was enacted following:

$$\theta_{EV} = \left\{ \begin{array}{ll} 2\pi - \arccos(PF_i), & \text{if } C_{EV,\mathcal{Z}_i} < 0 \\ \arccos(PF_i), & \text{if } C_{EV,\mathcal{Z}_i} > 0 \end{array} \right\}, \quad (7)$$

where PF_i is the power factor selected for each zone, i. The M2M optimization is applicable to both V2G and G2V cases.

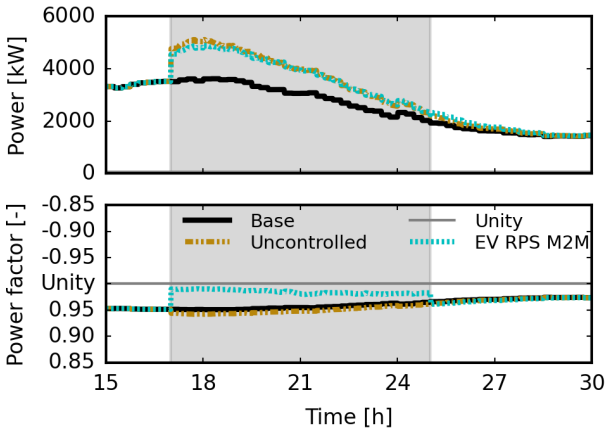

Fig. 8. The uncontrolled and RPS cases with 15% penetration of EVs, i.e. 260 cars, charging as they arrive home after 5pm. The RPS control time period for EV pf optimization was selected as 17-25:00h to improve the substation pf, thus, reducing losses during peak time, and mitigate voltage violations.

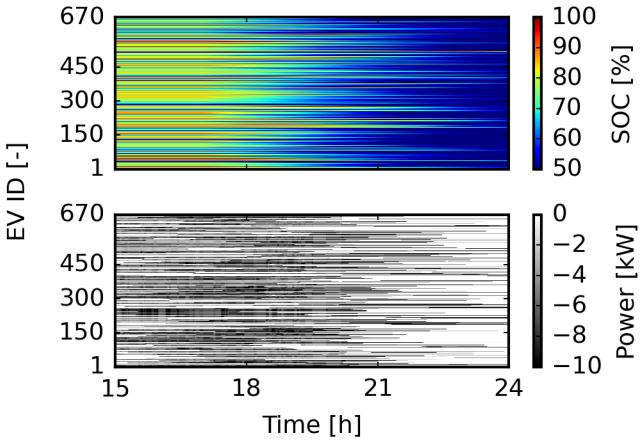

Fig. 9. The EV battery SOC (top) and variable power as determined by the RPS controls (bottom) during the V2G minutely simulation. All vehicles stop discharging at 50% SOC, sufficient for typical driving patterns based on NHTS survey daily driving distances.

V. Minute-to-Minute RPS Controls for V2G and Charging Case Studies

The M2M controls were applied first in V2G operation with 40% of the houses, i.e. 670, assumed to participate (Fig. 6). Solar PV at a penetration rate of 20% was considered in this future smart grid scenario in which the entire neighborhood load may be met from the DERs. In the period of 17:00 to 24:00, the vehicles with greater than 50% SOC discharge as they arrive home. In the uncontrolled case, the vehicles discharge at 10VA with a pf of 0.95 lagging, and the main feeder experiences reverse radial power flow and very low pf.

The pf switches from lagging to leading with the variation of solar PV generation and the number of participating vehicles for that time, t. From 17-18:00 the system load was completely supplied from the DERs, entirely alleviating the evening peak. During this time, the power factor drops to near zero when the reactive load is higher than the active load. Both behaviors

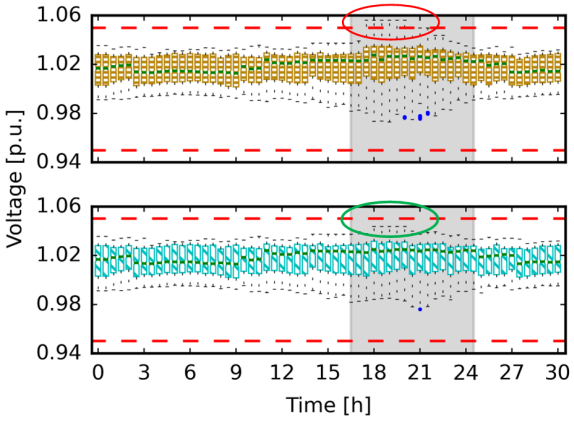

Fig. 10. The bus voltages across the system in the uncontrolled charging (top) and RPS cases with optimal phase angle selection (bottom). The voltage violations during the control window of 17-25:00 are successfully mitigated.

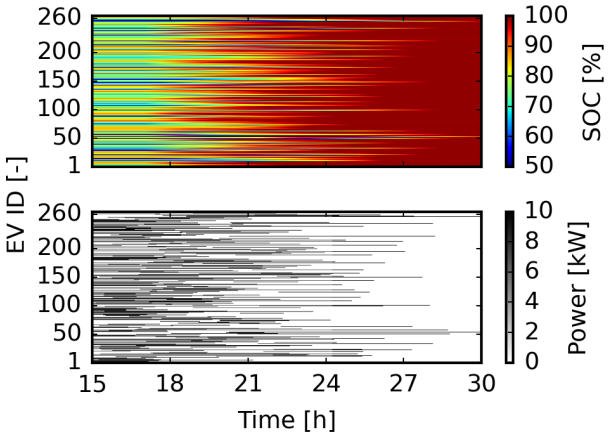

Fig. 11. The EV battery SOC (top) and variable power as determined by the RPS controls (bottom) during the G2V minutely simulation. Vehicles charge fully over a longer period time at reduced active power levels as determined by the RPS pf design selection.

represent major challenges to utilities to enact V2G at high penetrations or in resiliency scenarios where the entire load would be met from DERs.

To address these major challenges in the EV RPS M2M subcase, the optimization was solved with upper and lower EV pf bounds, $PF_{lag}, -PF_{lead}$, of 0.65 and -0.65 starting at 17:00. To limit the number of times the EV bi-directional chargers changed phase angle, each minute the previous design solution was simulated, and only if the main substation pf or system voltages violated acceptable thresholds of 1-0.9 lagging and 0.95-1.05p.u. would the optimization be repeated.

These controls maintained a near unity power factor as illustrated in Fig. 6, and less variation in the pf could be obtained by decreasing the allowed tolerance before repeating the optimization. The voltage during the V2G increases (Fig. 7), not to outside the limits, but the potential use case of RPS is further illustrated. This extreme use case was selected to show the capability of RPS to enable grid support scenarios, assuming the communication to send control signals to chargers and zones.

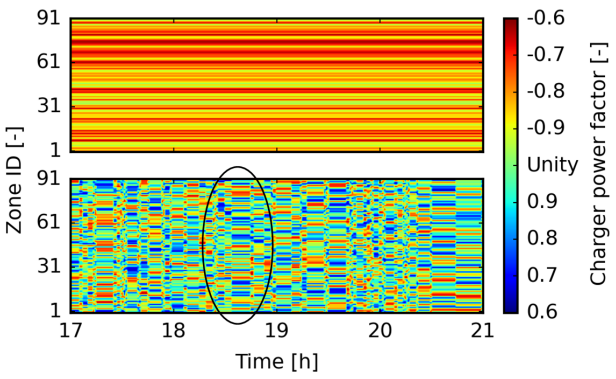

Fig. 12. The RPS control design selections for each zone's power factor in EV charging (top) and V2G (bottom). The initial design selection for the peak charging load was sufficient throughout the period and maintained. In V2G with reverse radial power flow and leading substation pf, updates are frequent.

In the second case for charging, a low EV penetration rate was employed and illustrated in Fig. 8, where 15% of the DS with 1,765 homes charge upon home arrival after 17:00. The EV RPS controls with upper and lower power factor bounds, $PF_{lag}, -PF_{lead}$, of 0.95 and -0.6 improve the substation power factor resulting in less losses on the system on the system and (Fig. 10). They also provide the major contribution of stopping significant bus voltage violations during peak additional charging load, as encircled.

In both the V2G and G2V scenarios, the individual SOC of each EV battery was modeled and considered (Fig. 9 and 11). Even with the reduced active power levels delivered to the EV batteries, all vehicles charge fully. The design solutions for RPS zonal EV pf in G2V and V2G cases as visualized in Fig. 12 determined the change in active power delivered to and from the EV battery.

The G2V design initial solution passed the threshold checks for the main substation pf and the voltage limits every minute and did not require updating in this example. In the V2G case study, the solution changed frequently because a higher penetration of EVs were considered, inclusion of variable solar PV, and intermittent reverse radial power flow. Encircled in Fig. 12 is a period where the optimization solution was maintained during which voltage rises but not to outside the limits as described in Fig. 7.

VI. Conclusion

A large-scale IEEE benchmark DS was modified to include 1,765 experimental residential smart meter profiles and hundreds of solar PV and EV modules and employed to study the proposed optimal controls for RPS. The framework enabled EV battery charging and discharging with RPS to substantially improve DS performance and reduce future need for additional smart capacitor installations. Specifically, in summer daily simulations with 20% solar PV and 15-40% EV penetration, the pf at the main substation feeder was corrected from leading and maintained within acceptable range of 0.9-1.0 lagging. The bus voltages were corrected to within 0.95-1.05p.u during charging, addressing a major concern of increased EV adoption rates. Minute-to-minute controls were enacted in both the V2G and G2V cases and the benefits of RPS for EV chargers showcased from a utility perspective.

Acknowledgment

This work was supported by the National Science Foundation (NSF) Graduate Research Fellowship under Grant No. 2239063. The support of the Leverhulme Trust under their visiting professorship scheme is also gratefully acknowledged. Any opinions, findings, and conclusions or recommendations expressed in this material are those of the authors and do not necessarily reflect the views of the sponsoring organizations. The authors are also grateful to the University of Kentucky L. Stanley Pigman Chair in Power endowment.

References

[1] Y. Cheng, H. Han, H. Wang, S. Chen, Y. Sun, and L. Fei, "Distributed control strategy based on line impedance identification for reactive power sharing in microgrid," in *2023 IEEE Energy Conversion Congress and Exposition (ECCE)*, 2023, pp. 1160–1167.

[2] H. Padullaparti, A. Pratt, I. Mendoza, S. Tiwari, M. Baggu, C. Bilby, and Y. Ngo, "Peak demand management and voltage regulation using coordinated virtual power plant controls," *IEEE Access*, vol. 11, pp. 130 674–130 687, 2023.

[3] M. Falahi, H.-M. Chou, M. Ehsani, L. Xie, and K. L. Butler-Purry, "Potential power quality benefits of electric vehicles," *IEEE Transactions on Sustainable Energy*, vol. 4, no. 4, pp. 1016–1023, 2013.

[4] J. Hu, C. Ye, Y. Ding, J. Tang, and S. Liu, "A distributed MPC to exploit reactive power V2G for real-time voltage regulation in distribution networks," *IEEE Transactions on Smart Grid*, pp. 576–588, 2022.

[5] J. Wang, G. R. Bharati, S. Paudyal, O. Ceylan, B. P. Bhattarai, and K. S. Myers, "Coordinated electric vehicle charging with reactive power support to distribution grids," *IEEE Transactions on Industrial Informatics*, vol. 15, no. 1, pp. 54–63, 2019.

[6] L. Wang, A. Dubey, A. H. Gebremedhin, A. K. Srivastava, and N. Schulz, "MPC-based decentralized voltage control in power distribution systems with ev and pv coordination," *IEEE Transactions on Smart Grid*, vol. 13, no. 4, pp. 2908–2919, 2022.

[7] Y. Wang, D. Qiu, G. Strbac, and Z. Gao, "Coordinated electric vehicle active and reactive power control for active distribution networks," *IEEE Transactions on Industrial Informatics*, vol. 19, pp. 1611–1622, 2023.

[8] D. A. Quijano, A. Padilha-Feltrin, and J. P. S. Catalão, "Volt-var optimization with power management of plug-in electric vehicles for conservation voltage reduction in distribution systems," *IEEE Transactions on Industry Applications*, vol. 60, no. 1, pp. 1454–1462, 2024.

[9] J. Sun, L. Zhu, R. Qin, D. J. Costinett, and L. M. Tolbert, "Single-phase gan-based t-type totem-pole rectifier with full-range zvs control and reactive power regulation," *IEEE Transactions on Power Electronics*, vol. 38, no. 2, pp. 2191–2201, 2023.

[10] H. Gong, V. Rallabandi, M. L. McIntyre, E. Hossain, and D. M. Ionel, "Peak reduction and long term load forecasting for large residential communities including smart homes with energy storage," *IEEE Access*, vol. 9, pp. 19 345–19 355, 2021.

[11] F. H. Administration, "National Household Travel Survey," 2017, https://nhts.ornl.gov/.

[12] H. Gong, R. E. Alden, and D. M. Ionel, "Stochastic battery SOC model of EV community for V2G operations using CTA-2045 standards," in *2022 IEEE Transportation Electrification Conference & Expo (ITEC)*, 2022, pp. 1144–1147.

[13] P. Meira, "DSS-python," 2022. [Online]. Available: https://pypi.org/project/dss-python/0.12.1/

[14] S. S. G. Acharige, M. E. Haque, M. T. Arif, N. Hosseinzadeh, K. N. Hasan, and A. M. T. Oo, "Review of electric vehicle charging technologies, standards, architectures, and converter configurations," *IEEE Access*, vol. 11, pp. 41 218–41 255, 2023.

[15] T. Gonen, *Electric Power Distribution Engineering (3rd ed.)*. CRC press, 2014.

[16] "Distribution capacitor automation," 2009. [Online]. Available: https://documents.dps.ny.gov/public/Common/ViewDoc.aspx?DocRefId=%7BE19FC0CA-EEDA-4AA6-82F9-D7B06AD36750%7D

[17] J. Blank and K. Deb, "Pymoo: Multi-objective optimization in python," *IEEE Access*, vol. 8, pp. 89 497–89 509, 2020.